

# Spatial analysis of Cdc42 activity reveals a role for plasma membrane-associated Cdc42 in centrosome regulation

Kari A. Herrington<sup>a</sup>, Andrew L. Trinh<sup>b</sup>, Carolyn Dang<sup>a</sup>, Ellen O'Shaughnessy<sup>c</sup>, Klaus M. Hahn<sup>c</sup>, Enrico Gratton<sup>a,b,d</sup>, Michelle A. Digman<sup>a,b,d</sup>, and Christine Sütterlin<sup>a,\*</sup>

<sup>a</sup>Department of Developmental and Cell Biology and <sup>b</sup>Department of Biomedical Engineering, University of California, Irvine, Irvine, CA 92697; <sup>c</sup>Department of Pharmacology, University of North Carolina at Chapel Hill, Chapel Hill, NC 27599; <sup>d</sup>Centre for Bioactive Discovery in Health and Ageing, School of Science and Technology, University of New England, Armidale, NSW 2351, Australia

**ABSTRACT** The ability of the small GTPase Cdc42 to regulate diverse cellular processes depends on tight spatial control of its activity. Cdc42 function is best understood at the plasma membrane (PM), where it regulates cytoskeletal organization and cell polarization. Active Cdc42 has also been detected at the Golgi, but its role and regulation at this organelle are only partially understood. Here we analyze the spatial distribution of Cdc42 activity by monitoring the dynamics of the Cdc42 FLARE biosensor using the phasor approach to FLIM-FRET. Phasor analysis revealed that Cdc42 is active at all Golgi cisternae and that this activity is controlled by Tuba and ARHGAP10, two Golgi-associated Cdc42 regulators. To our surprise, FGD1, another Cdc42 GEF at the Golgi, was not required for Cdc42 regulation at the Golgi, although its depletion decreased Cdc42 activity at the PM. Similarly, changes in Golgi morphology did not affect Cdc42 activity at the Golgi but were associated with a substantial reduction in PM-associated Cdc42 activity. Of interest, cells with reduced Cdc42 activity at the PM displayed altered centrosome morphology, suggesting that centrosome regulation may be mediated by active Cdc42 at the PM. Our study describes a novel quantitative approach to determine Cdc42 activity at specific subcellular locations and reveals new regulatory principles and functions of this small GTPase.

## Monitoring Editor

Rong Li  
Johns Hopkins University

Received: Sep 19, 2016

Revised: May 5, 2017

Accepted: May 15, 2017

## INTRODUCTION

Tight spatial regulation of the small Rho GTPase Cdc42 is required for many cellular processes, including cell polarity, cell survival, adhesion, migration, cell cycle progression, and membrane trafficking (Coso *et al.*, 1995; Nobes and Hall, 1995; Kroschewski *et al.*, 1999; Etienne-Manneville and Hall, 2001). Each of these functions depends on regulated localization and activation of Cdc42, which is achieved through its recruitment to a specific cellular membrane. Membrane association of Cdc42 is necessary for its activation and

requires the modification of its C-terminal end with a geranylgeranyl anchor (Michaelson *et al.*, 2001). Activation is catalyzed by guanine nucleotide exchange factors (GEFs) and guanine nucleotide dissociation inhibitors (GDIs), which assist in the translocation between the membrane and cytosol (Ku *et al.*, 2001; Michaelson *et al.*, 2001; Salazar *et al.*, 2003; Egorov *et al.*, 2009). Membrane trafficking has also been found to be critical for control of Cdc42 localization and activation (Osmani *et al.*, 2010).

This article was published online ahead of print in MBoc in Press (<http://www.molbiolcell.org/cgi/doi/10.1091/mboc.E16-09-0665>) on May 24, 2017.

K.A.H. and C.S. conceived and designed the experiments; K.A.H. performed the experiments; K.A.H. analyzed the data; K.A.H., K.M.H., E.G., M.A.D., and C.S. drafted the article; K.A.H. prepared the digital images; A.L.T. performed migration experiments; C.D. aided with cloning and data analysis; E.O. developed the Cdc42-FLRE biosensor; K.M.H. provided the Cdc42-FLARE biosensor; E.G. provided FLIM-FRET expertise; M.A.D. provided microscope and FLIM-FRET expertise.

\*Address correspondence to: Christine Sütterlin ([suetterc@uci.edu](mailto:suetterc@uci.edu)).

Abbreviations used: CBD, Cdc42-binding domain; FLIM, fluorescence lifetime imaging; FRET, Förster resonance energy transfer; GAP, GTPase-activating protein; GDI, guanine nucleotide dissociation inhibitor; GEF, guanine nucleotide exchange factor; ManII, mannosidase II; PM, plasma membrane.

© 2017 Herrington *et al.* This article is distributed by The American Society for Cell Biology under license from the author(s). Two months after publication it is available to the public under an Attribution-Noncommercial-Share Alike 3.0 Unported Creative Commons License (<http://creativecommons.org/licenses/by-nc-sa/3.0>). "ASCB," "The American Society for Cell Biology," and "Molecular Biology of the Cell" are registered trademarks of The American Society for Cell Biology.

Cdc42 is proposed to be a functional component of the Golgi. The localization of this small GTPase to the Golgi was detected with diverse methods, including fractionation, immunofluorescence, and electron microscopy (Erickson *et al.*, 1996; Luna *et al.*, 2002; Matas *et al.*, 2004; Osmani *et al.*, 2010). Golgi-associated Cdc42 is active, as observed directly through biosensor experiments and indirectly through visualization of the Cdc42 effectors Arp2/3 and N-Wiskott-Aldrich syndrome protein (N-WASP) at the Golgi (Luna *et al.*, 2002; Nalbant *et al.*, 2004; Dubois *et al.*, 2005; Baschieri *et al.*, 2014). Cdc42 at the Golgi has been implicated in typical Golgi functions because disrupting its activity caused defects in protein transport through the Golgi (Wu *et al.*, 2000; Luna *et al.*, 2002; Egorov *et al.*, 2009; Hehnlly *et al.*, 2009; Park *et al.*, 2015). It has also been linked to the regulation of centrosome organization and function (Kodani *et al.*, 2009). However, it is not clear whether the Golgi-associated pool of Cdc42 is controlling these processes because it has not been possible to selectively disrupt the activity of this specific protein population.

Several factors have been implicated in the regulation of Cdc42 activity at the Golgi. Two Cdc42-specific GEFs, Tuba and FGD1, are reported to localize to the Golgi. Tuba was observed at the Golgi in rat brain cryosections and in the perinuclear region of HeLa cells (Salazar *et al.*, 2003; Kodani *et al.*, 2009), and FGD1 localized to the *trans*-Golgi of HeLa, COS-7, and MC3T3 osteoblasts (Estrada *et al.*, 2001; Egorov *et al.*, 2009). Golgi membranes also host the Cdc42-specific GTPase-activating protein (GAP) ARHGAP10 (Dubois *et al.*, 2005). In addition, GM130 and coronin7, two resident Golgi proteins without typical GEF and GAP domains, are proposed to contribute to Cdc42 regulation at the Golgi (Kodani *et al.*, 2009; Bhattacharya *et al.*, 2016). Biochemical assays in total cell lysates showed that GM130 controls ~50% of cellular Cdc42 activity (Kodani *et al.*, 2009). This peripheral Golgi protein is proposed to contribute to Cdc42 regulation by binding and sequestering RasGRF2, a Ras GEF that binds inactive Cdc42 at the plasma membrane (Calvo *et al.*, 2011; Baschieri *et al.*, 2014). Coronin7, in contrast, may limit Cdc42 activity at the Golgi. Its loss resulted in excessive N-WASP-mediated actin polymerization at the Golgi and a disrupted Golgi phenotype (Bhattacharya *et al.*, 2016). In spite of these studies, it remains unclear whether these regulatory proteins actually contribute to the control of Cdc42 activity at the Golgi.

Several methods have been developed to detect intracellular Cdc42 activity. Biochemical assays, such as the PAK-CRIB binding assay, reveal the level of Cdc42 activity in total cell lysates (Benard and Bokoch, 2002). They use specific effector domains to isolate activated, GTP-bound Cdc42 molecules but have the disadvantage of not providing any spatial information. Förster resonance energy transfer (FRET) biosensors provide spatial information on the activity of small GTPase such as Cdc42 inside a cell (Machacek *et al.*, 2009; Kunida *et al.*, 2012; Nalbant *et al.*, 2004; Itoh *et al.*, 2002). However, the commonly used Cdc42 biosensors have limitations. The MeroCBD probe described by Nalbant *et al.* (2004) is an elegant tool to study Cdc42 activity in living cells but requires synthesis of dyes and cell loading through microinjection. Although this probe has demonstrated the presence of active Cdc42 at the Golgi, it is impractical for routine use. Genetically encoded FRET biosensors are easier to use because they can be expressed transiently or stably. In the Cdc42 FLARE biosensor used here, the Cdc42 C-terminus is free to interact with GDI and undergo the geranylgeranyl modification that is essential for physiologically correct regulation of its activity (Michaelson *et al.*, 2001; Itoh *et al.*, 2002; Machacek *et al.*, 2009; Hanna *et al.*, 2014).

Fluorescence lifetime imaging (FLIM) is a powerful method to measure FRET. It detects the specific rate of fluorescence decay, or lifetime, of only the donor fluorophore, which is constant unless an acceptor fluorophore is close enough to absorb the emitted energy, for example, when FRET occurs (Elangovan *et al.*, 2002). FLIM is superior to traditional intensity-based ratiometric methods because it eliminates fluorescence artifacts inherent to biosensor design, which may lead to false measurements of Rho GTPase activity (Wallrabe and Periasamy, 2005; Hinde *et al.*, 2012). For example, FRET detection by FLIM eliminates the effects of variations in biosensor concentration on activity measurements (Hinde *et al.*, 2012). FLIM measurements also avoid issues with spectral bleedthrough, channel alignment, and photobleaching (Chen *et al.*, 2003; Wallrabe *et al.*, 2006). Because the fluorescence lifetime is sensitive to changes in the cellular environment, FLIM can be performed in living cells, which avoids fixation artifacts (Michaelson *et al.*, 2001; Chen *et al.*, 2003; Wallrabe and Periasamy, 2005). In addition, FLIM can readily differentiate between different fluorophore species and generate quantitative maps showing the average fraction of molecules at a given location that are undergoing FRET (Hinde *et al.*, 2012).

FLIM data can be readily analyzed using the phasor approach, which describes the transformation of the numerous exponential fluorescence decay curves of each pixel into a two-dimensional plot called the phasor plot (Digman *et al.*, 2008). This transformation plots each pixel to a unique place on the phasor plot according to lifetime. Because the phasor plot is directly linked to the image, it allows the mapping of the lifetimes back to the image to provide a clear view of spatial changes in lifetime within the image. Overall, the phasor approach to FLIM simplifies the analysis of large FLIM data sets and provides a global view of FLIM data inside a cell.

This study aimed at identifying factors that control Cdc42 activity at the Golgi. Using the phasor approach to FLIM-FRET, we show that the activity of Cdc42, which was present throughout the Golgi, was regulated by ARHGAP10 and Tuba but not FGD1. Although Cdc42 activity at the Golgi was independent of Golgi structure, a connected Golgi ribbon was necessary for Cdc42 activity at the plasma membrane (PM). Finally, we found that Cdc42 activity at the PM, not the Golgi, contributed to the control of centrosome organization and function.

## RESULTS

### Spatial detection of Cdc42 activity using the phasor approach to FLIM-FRET

We generated a stable cell line expressing the Cdc42-FLARE biosensor, which employs the cerulean/YPet FRET pair in a dual-chain design (donor fluorophore on the N-terminus of Cdc42, acceptor fluorophore YPet on the CRIB domain of the Cdc42 effector N-WASP; Figure 1A). To avoid excessive expression of the biosensor and achieve similar expression levels in all cells, we generated a stable clonal U2OS (human osteosarcoma) cell line that expresses Cdc42-FLARE from an inducible promoter. Induction for 48 h resulted in expression levels of the biosensor that were about eightfold higher than those of endogenous protein (Supplemental Figure S1A) but did not affect cell morphology or function (Supplemental Figures S1B and S2). The imaging cell line also constitutively expressed the Golgi protein mannosidase II (ManII) fused to mCherry to label the medial-Golgi cisternae (Figure 1B). We routinely induced this imaging cell line for 48 h, which led to an enrichment of cerulean-Cdc42 at the Golgi, as previously reported (Erickson *et al.*, 1996; Michaelson *et al.*, 2001). To evaluate

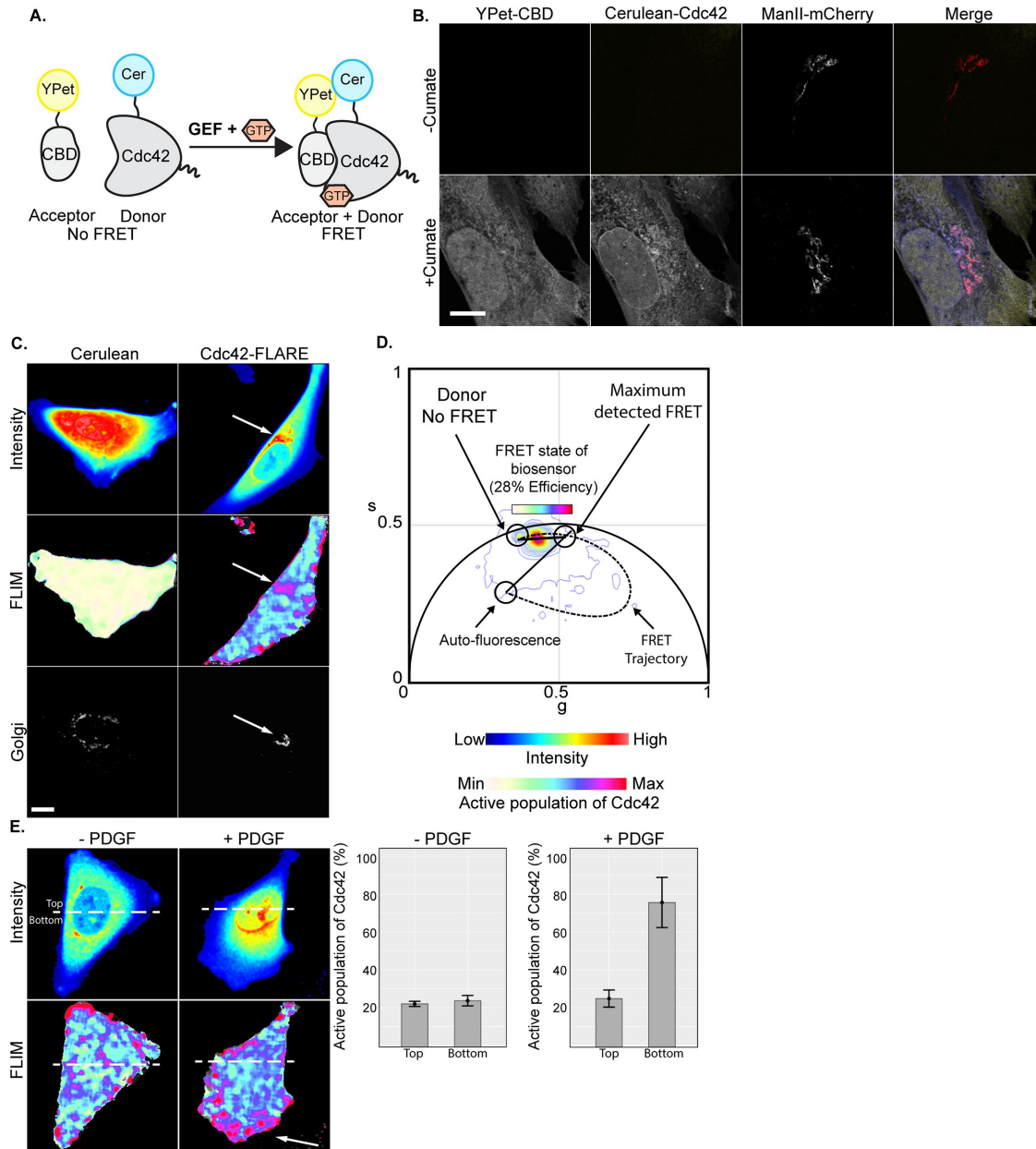


**FIGURE 1:** Cdc42 activity inside a cell can be visualized with the phasor approach to FLIM-FRET. (A) Dual-chain biosensor Cdc42-FLARE with the FRET pair cerulean-Cdc42 and YPet-CBD in its inactive and active state. (B) The stable U2OS-Cdc42-FLARE cell line, which inducibly expresses Cdc42-FLARE while constitutively expressing ManII-mCherry, was left uninduced (top) or induced with cumate for 48 h (bottom). Confocal images of representative cells. (C) Intensity and FLIM maps of a control cell, which expresses the cerulean donor alone, or a U2OS-Cdc42-FLARE cell after induction for 48 h. The intensity maps (top) use a blue (low intensity) to red (high intensity) scale to show the distribution of cerulean (left) or cerulean-Cdc42 (right). The FLIM maps (middle) show the active population of the biosensor in the range from 0% (white) to a maximal FRET of 28% (magenta), as calculated from the cerulean lifetimes through the phasor plot shown in D. (D) Phasor plot of the distribution of cerulean lifetimes for the cells from C with the superimposed theoretical FRET trajectory, calculated with the SIM-FCS software. (E) FLIM-FRET analysis of Cdc42 activity in nonmigrating and migrating cells. U2OS-Cdc42-FLARE imaging cells, after cumate induction for 48 h, were left untreated (left) or incubated with PDGF to stimulate migration (right). Intensity maps of cerulean-Cdc42 are shown, as well as FLIM maps that reflect the fraction of the active Cdc42 population. The graphs show a quantification of the percentage of active Cdc42 molecules in the top or bottom half of unstimulated and stimulated cells.

donor and acceptor concentrations under these experimental conditions, we analyzed cells by cross-raster image correlation spectroscopy (ccRICS), a fluctuation method that detects protein complexes that are mobile and diffusing together. ccRICS revealed that donor and acceptor protein concentrations were high

enough to allow an interaction between these two proteins and fairly constant between samples (unpublished data). For this entire study, we focused on cells with a maximum of one to three neighboring cells, so the majority of its PM was not in contact with other cells.

Inducible expression of Cdc42-FLARE did not alter cell morphology and behavior. A comparison of wild-type U2OS and uninduced and induced U2OS-Cdc42-FLARE cells in an immunofluorescence analysis showed no difference in the organization of the endoplasmic reticulum (ER), Golgi, and cytoskeleton (Supplemental Figure S1B). In addition, Cdc42-dependent functions, such as anterograde and retrograde protein transport at the Golgi, as well as filopodia formation, were unaffected by expression of this biosensor (Supplemental Figure S2, A and B). Finally, the organization of the centrosome, which we reported to be altered in cells with reduced Cdc42 activity, was normal (Supplemental Figure S1B; Kodani et al., 2009).

We used the phasor approach to FLIM-FRET to detect the activity of this biosensor at the Golgi and the PM. We first defined the range of FRET efficiencies in cells. The intensity map of cells expressing cerulean in the absence of an acceptor showed greater intensity in the center of the cell (Figure 1C, left, blue-to-red scale). Because FLIM is independent of fluorophore concentration, the fluorescence lifetime of cerulean was uniform (Figure 1C, middle), corresponding to  $\sim 2.8$  ns on the universal semicircle of the phasor plot (Digman et al., 2008), and was quenched to a maximum of  $\sim 1.9$  ns. The elliptical trajectory shown in the phasor plot coordinates indicates that the

maximal detected FRET efficiency was 28% for our experimental conditions (Figure 1D). Given that this biosensor is either on or off, the line that connects the high FRET ("on") state to the no FRET ("off") state of the phasor describes the fractional population of the active biosensor. In this study, the results are reported as the fraction of active Cdc42 molecules, with 0% showing no active small GTPase and 100% indicating the highest detectable fraction of active Cdc42. Cerulean-Cdc42 was enriched in the perinuclear region of Cdc42-FLARE-expressing cells, where it colocalized with the Golgi marker ManII-mCherry (Figure 1C, right). In these cells, the fraction of active Cdc42 molecules was highest at the Golgi and PM compared with the rest of the cell (Figure 1D; Hinde et al., 2012). These data are consistent with reports by the Hahn lab with the MeroCBD biosensor, which detected activity of endogenous Cdc42 at the Golgi in nonpolarized cells (Nalbant et al., 2004).

We validated our assay by monitoring Cdc42 activity at the leading edge of polarized cells, a well-established site of active Cdc42 (Nalbant et al., 2004; Monypenny et al., 2009; Hanna et al., 2014). We stimulated cell polarization and migration in collagen I-coated chemotaxis chambers using platelet-derived growth factor (PDGF) and performed FLIM-FRET measurements. As expected, there was high FRET at the leading edge of the cell (arrow) during cell migration, which was absent from unstimulated control cells (Figure 1E and Supplemental Figure S3). Similarly, higher levels of FRET were also detected throughout cells that transiently expressed a constitutively active form of the Cdc42-FLARE biosensor compared with the wild-type biosensor (Supplemental Figure S4).

We next monitored Cdc42 activity at individual Golgi cisternae. We generated additional U2OS cell lines that inducibly expressed Cdc42-FLARE together with low levels of specific *cis*- or *trans*-Golgi markers (Figure 2A). To increase the resolution at the Golgi, we focused on a  $25.29 \times 25.29 \mu\text{m}^2$  region ( $\sim 100$  nm/pixel), which we found to be the smallest area to contain most Golgi membranes. Cdc42-FLARE was enriched at the Golgi in each of the cell lines. To isolate Cdc42 activity at each individual Golgi cisternae, we overlaid the FLIM data with a mask of Golgi cisternae-specific markers, which we generated by thresholding images of mApple-p58, ManII-mCherry, or GalT-mCherry recorded in parallel. This approach revealed similar average fractions of active Cdc42 of 76.98, 74.13, and 73.8% at the *cis*-Golgi (mApple-p58), medial-Golgi (ManII-mCherry), and *trans*-Golgi (GalT-mCherry), respectively.

To increase the resolution at the Golgi, we focused on a  $25.29 \times 25.29 \mu\text{m}^2$  region ( $\sim 100$  nm/pixel), which we found to be the smallest area to contain most Golgi membranes. Cdc42-FLARE was enriched at the Golgi in each of the cell lines. To isolate Cdc42 activity at each individual Golgi cisternae, we overlaid the FLIM data with a mask of Golgi cisternae-specific markers, which we generated by thresholding images of mApple-p58, ManII-mCherry, or GalT-mCherry recorded in parallel. This approach revealed similar average fractions of active Cdc42 of 76.98, 74.13, and 73.8% at the *cis*-Golgi (mApple-p58), medial-Golgi (ManII-mCherry), and *trans*-Golgi (GalT-mCherry), respectively. These experiments show that the Cdc42-FLARE biosensor with the phasor approach to FLIM-FRET is capable of detecting enrichment in active Cdc42 at the leading edge and all Golgi cisternae.

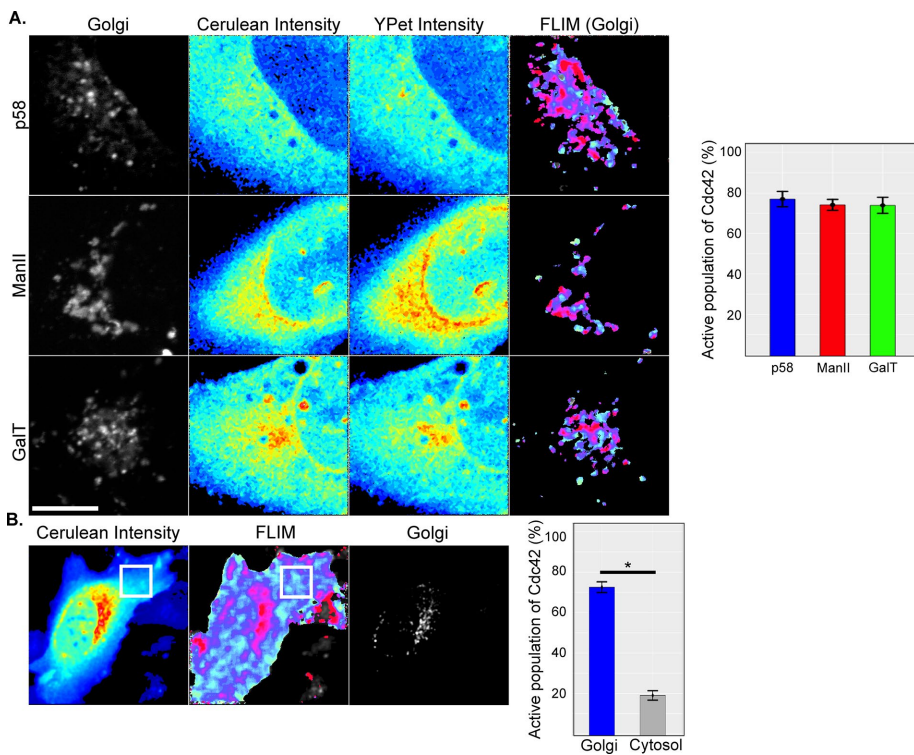


**FIGURE 2:** FLIM-FRET measurements detect Cdc42 activity at the Golgi. (A) Cdc42 activity measurements in a  $25.29 \times 25.29 \mu\text{m}^2$  square containing the *cis*-, medial-, or *trans*-Golgi cisternae in U2OS-Cdc42-FLARE imaging cell lines constitutively expressing p58-mApple, ManII-mCherry or GalT-mCherry, respectively (left). Intensity maps for cerulean-Cdc42 and YPet in this region (middle two) are also shown. The percentages of active Cdc42 at specific Golgi cisternae were determined by overlaying FLIM maps with thresholded images of each Golgi marker (right). Graph shows the average percentage of active Cdc42 at each Golgi cisternae from eight cells per experiment and three independent experiments. (B) A comparison of Cdc42 activity at the Golgi and a random area in the cytosol. For a representative U2OS-Cdc42-FLARE imaging cell, the cerulean intensity (left) and the FLIM map (middle) are shown for the entire cell. Expression of ManII-mCherry (right) was used to mark the Golgi so that the specific FLIM signal at this location could be extracted. The position of the area in the cytosol ( $11.8 \times 11.8 \mu\text{m}^2$ , halfway between the perinuclear region and the PM) is shown as boxes in the intensity and FLIM maps. Scale bar, 10  $\mu\text{m}$ . Graph shows the average percentage of active Cdc42 at the Golgi or in the cytosol from 8–12 cells per experiment and three independent experiments. \* $p < 0.0001$ .

### Golgi-associated Cdc42 regulators have differential roles in controlling Cdc42 activity at the Golgi

We used the U2OS-Cdc42-FLARE cell line to investigate the role of the Golgi-associated GAP ARHGAP10 in the regulation of Cdc42 activity at the Golgi. This protein has been implicated in Cdc42 regulation at the Golgi through indirect measurements of protein transport (Dubois *et al.*, 2005). Consistent with published data, a truncated form that only contains the PH and GAP domains but lacks the PM targeting domain localized to the Golgi in our imaging cell line (Figure 3A and Supplemental Figure S5; Dubois *et al.*, 2005). FLIM-FRET analysis in cells expressing this construct revealed a significant decrease in Cdc42 activity at the Golgi, with a reduction in the percentage of active Cdc42 from 71.46 to 49.2% ( $t(52) = 18.1771$ ,  $p < 0.0001$ ; Figure 3B). This reduction was not due to effects on donor or acceptor levels because fluorescence intensities of these proteins were similar in both samples (Supplemental Figure S5). We conclude that the Golgi-associated pool of ARHGAP10 is able to inactivate Cdc42 at the Golgi and provide the first direct evidence that manipulations of a Cdc42 regulator lead to a decrease in Golgi-associated Cdc42 activity.

We next examined whether activation of Cdc42 at the Golgi depends on Tuba, which is reported to associate with the Golgi and the PM. We transfected U2OS-Cdc42-FLARE imaging cells with either control (scrambled) or Tuba-specific small interfering RNA (siRNA) and collected FLIM data at the Golgi, which was marked by ManII-mCherry. We also collected FLIM data at the PM, which was labeled by expression of the PM marker mApple-farnesyl. For this experiment, we zoomed in on the PM to the same extent as the Golgi, focusing on a region of the PM not in contact with other cells. After data collection, we verified protein loss in the cells that we had imaged through immunofluorescence analysis on gridded dishes (Supplemental Figure S6). Tuba-depleted cells contained a much smaller fraction of active Cdc42 at the Golgi and the PM than control cells, with decreases from 72.7 to 52.1% ( $t(52) = 9.9833$ ,  $p < 0.0001$ ) and 70.2 to 49.9% ( $t(56) = 14.9569$ ,  $p < 0.0001$ ), respectively (Figure 4, A and B).

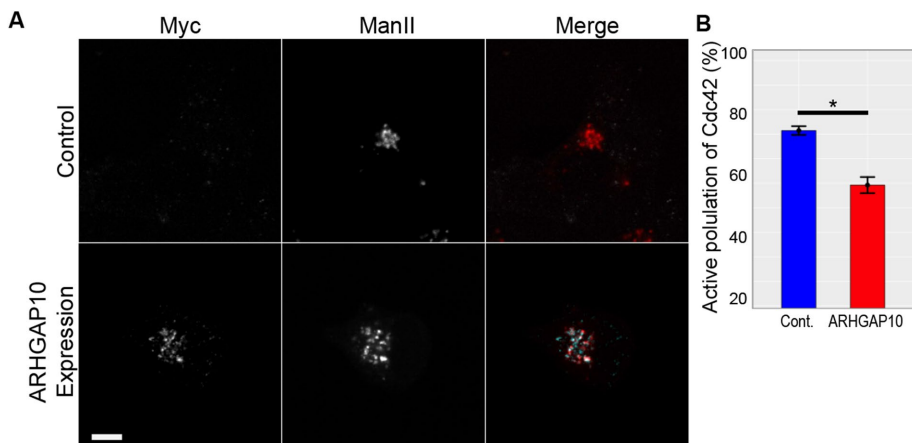


**FIGURE 3:** ARHGAP10 controls Cdc42 activity at the Golgi. A construct encoding for a myc-tagged ARHGAP10 truncation consisting of the PH and GAP domains, which mediate Golgi localization, was transfected into the U2OS-Cdc42-FLARE imaging cell line that constitutively expresses ManII-mCherry. The percentages of active Cdc42 were determined with the phasor approach to FLIM-FRET, as described in Figure 1. (A) For each cell that was analyzed by FLIM-FRET, the association of the ARHGAP10 truncation with the Golgi (marked by ManII-mCherry) was verified through immunofluorescence staining with antibodies to myc. (B) Average percentage of active Cdc42 at the Golgi from cells that either express an empty vector (Cont.) or Golgi-targeted ARHGAP10. At least eight cells were analyzed per experiment, and three independent experiments were performed. \* $p < 0.0001$ .

We performed a similar analysis for Golgi-localized Cdc42 GEF FGD1 (Estrada *et al.*, 2001), which was found to be necessary for Golgi-to-PM transport (Egorov *et al.*, 2009). To our surprise, the fraction of active Cdc42 at the Golgi was similar in control and FGD1-depleted cells—74.28 and 73%, respectively. However, there was a reduction in the percentage of active Cdc42 at the PM from 73.9% in control cells to 51.9% in FGD1-depleted cells ( $t(36) = 5.8322$ ,  $p < 0.0001$ ; Figure 4B and Supplemental Figure S6). Thus, in spite of its Golgi association, this Cdc42 GEF does not appear to contribute to Cdc42 activation at the Golgi. For this entire set of experiments, we verified that our manipulations did not affect fluorescence intensities of donor and acceptor proteins (Supplemental Figure S6).

### Ribbon-like Golgi organization is important for Cdc42 activation at the PM

We next measured Cdc42 activity in cells with altered Golgi organization. The Golgi ribbon was reported to be maintained by the structural Golgi protein GM130, with GM130 loss leading to disconnected Golgi stacks (Puthenveedu *et al.*, 2006). GM130 was depleted from the U2OS-Cdc42-FLARE imaging cell lines, followed by Cdc42 activity measurements with our FLIM-FRET assay. We then fixed the cells and stained them with an antibody to GM130 to confirm protein depletion in the cells that we had imaged. To our surprise, the fractions of active Cdc42 at the Golgi were similar in control and GM130-depleted cells—70.4 and 71.8%, respectively (Figure 5A and Supplemental Figure S7). However, at the PM of these cells, there was a significant decrease in the fraction of active Cdc42, from 69.0 to 50.8% ( $t(40) = 8.9123$ ,  $p < 0.0001$ ), which was not observed in control cells. This effect was specific and not due to reduced levels of donor or acceptor molecules (Supplemental Figure S7). This result suggests that either GM130 or Golgi ribbon organization is important for Cdc42 activation at the PM.

To differentiate between these possibilities, we analyzed cells with an extensively fragmented Golgi. We focused on golgin-84, a structural Golgi protein whose loss leads to Golgi fragmentation, dispersal, and a reduction in protein transport (Diao *et al.*, 2003).

Control and golgin-84-depleted cells showed similar FRET percentages at the Golgi (Figure 5B and Supplemental Figure S7) but not at the PM, where golgin-84 depletion caused a decrease in the fraction of active Cdc42 from 69.82 to 45.17% ( $t(38) = 11.1093$ ,  $p < 0.0001$ ). These results suggest that Cdc42 activation at the Golgi is independent of Golgi organization but that disruption of Golgi organization prevents Cdc42 activation at the PM.

### Cdc42 controls centrosome organization from the PM

We next tested whether Cdc42 activity at the PM is critical for the regulation of the centrosome. We previously reported centrosome abnormalities in cells in which total cellular Cdc42 activity was reduced through depletion of GM130 or Tuba or overexpression of dominant-negative Cdc42 (Kodani *et al.*, 2008, 2009). We focused our analysis on FGD1- and golgin-84-depleted cells because they displayed reduced Cdc42 activity only at the PM (Figures 4 and 5). As a readout for centrosome organization, we

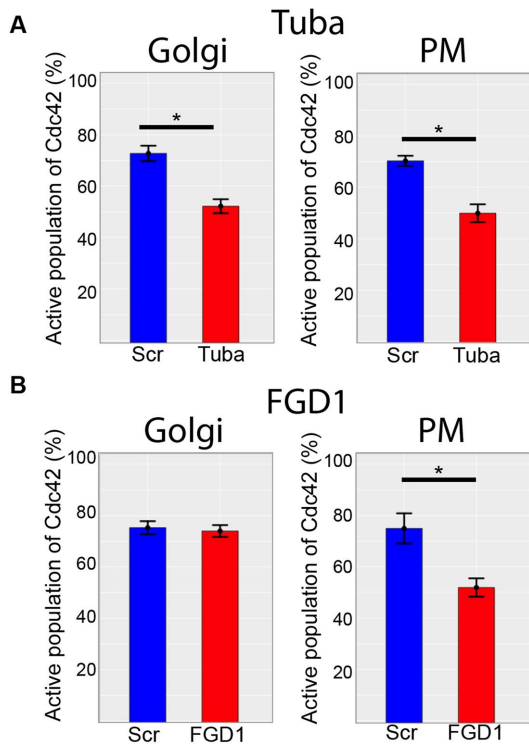


**FIGURE 4:** Tuba, but not FGD1, regulates Cdc42 activity at the Golgi. FLIM-FRET analysis of cells lacking the Golgi-associated GEFs Tuba or FGD1. The U2OS-Cdc42-FLARE imaging cell line, which also expressed ManII-mCherry or mApple-farnesyl to label the Golgi or PM, respectively, was transfected with scrambled-, Tuba-, or FGD1-specific siRNA and subjected to FLIM-FRET analysis at the Golgi or PM. Average percentage of active Cdc42 at the Golgi (left) or the PM (right). For each condition, eight cells were analyzed per experiment, and three independent experiments were performed. \* $p < 0.0001$ . (A) FLIM-FRET analysis of scrambled (Scr) and Tuba-depleted cells (Tuba). (B) FLIM-FRET analysis of scrambled (Scr) and FGD1-depleted cells (FGD1).

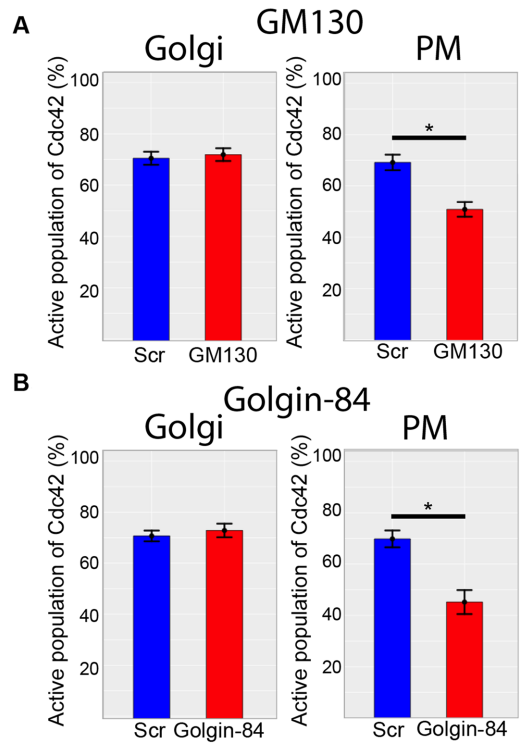


**FIGURE 5:** Cdc42 activity at the PM depends on normal Golgi organization. The phasor approach to FLIM-FRET was used to determine Cdc42 activity at the Golgi and PM after disruption of Golgi organization through depletion of GM130 and golgin-84. Cdc42 activity measurements at the Golgi and PM were performed in induced U2OS-Cdc42-FLARE cells expressing ManII-mCherry or mApple-farnesyl. Average percentage of active Cdc42 at the Golgi (left) and the PM (right). For each condition, eight cells were analyzed per experiment, and three independent experiments were performed. \* $p < 0.0001$ . (A) FLIM-FRET measurements of cells treated with control (Scr) or GM130-specific siRNA. (B) FLIM-FRET measurements of cells transfected with scrambled (Scr) or golgin-84-specific siRNA (Golgin-84).

monitored the centrosomal protein kendrin, which reveals centrosome abnormalities in cells with reduced Cdc42 activity (Kodani *et al.*, 2009). Whereas control cells displayed the typical complement of two to four centrioles, there were aberrant kendrin foci next to the centrioles in FGD1- and golgin-84-depleted cells (Figure 6B, right).  $\gamma$ -Tubulin organization, in contrast, was unaltered, which is consistent with earlier reports (Kodani *et al.*, 2009). Thus, because golgin-84- and FGD1-depleted cells phenocopied the centrosome defects of GM130-depleted cells (Figure 6, B and C), we conclude that Cdc42 activity at the PM, and not the Golgi, may be critical for the maintenance of proper centrosome organization.

## DISCUSSION

This study provides new insights into the control of Cdc42 activity at different cellular locations. The use of a dual-chain FRET biosensor and the phasor approach to FLIM led to three novel findings with regard to the spatial regulation and function of Cdc42 activity. We show that 1) Golgi-associated Cdc42 activity is controlled by ARHGAP10 and Tuba but not FGD1 and GM130, 2) Cdc42 activity at the PM depends on an intact Golgi ribbon, and 3) PM-associated Cdc42 activity is critical for the organization and function of the centrosome.

We used novel tools to map Cdc42 activity in living cells. We established stable U2OS imaging cell lines for Cdc42 activity measurements, which inducibly expressed the Cdc42-FLARE biosensor. These imaging cell lines also expressed Golgi and PM markers, which facilitated measurement of Cdc42 activity at these specific locations at high pixel resolution ( $25.29 \times 25.29 \mu\text{m}^2$ ;  $\sim 100 \text{ nm/pixel}$ ). We measured FRET with the phasor approach to FLIM in live cells, which allowed us to obtain quantitative measures of Cdc42 activity at specific cellular locations. There were approximately four times more active Cdc42 molecules at the Golgi than in randomly selected areas in the cytosol.

FLIM-FRET is highly suitable for this study because artifacts that are either caused by sample fixation or inherent to ratiometric FRET measurements were avoided. It also allowed for the detection of Cdc42 activity in areas with low biosensor expression levels. This became evident in migration experiments, in which the increase in the percentage of active Cdc42 molecules at the leading edge was not caused by a change in cerulean-Cdc42 intensity.

Our study is the first to provide direct support for the differential regulation of Cdc42 activity at the Golgi and PM in live cells. At the Golgi, Cdc42 activity was down-regulated when we expressed a Golgi-targeted form of ARHGAP10 or depleted Tuba. At the PM, Cdc42 activity was reduced when FGD1 was removed or Golgi

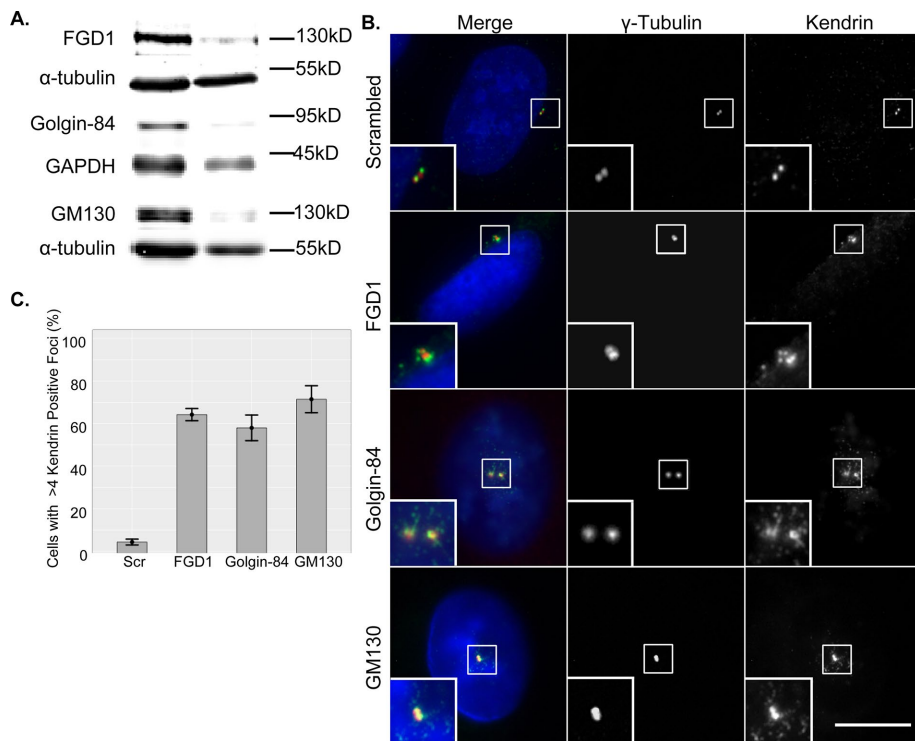


**FIGURE 6:** Active Cdc42 at the PM is necessary for the control of normal centrosome organization. (A) Western blot of total cell lysates from U2OS cells transfected with scrambled siRNA as a negative control (left) or siRNA specific to FGD1, golgin-84, or GM130 for 48 h (right).  $\alpha$ -Tubulin and glyceraldehyde 3-phosphate dehydrogenase served as loading controls. (B) Cells from A were analyzed by immunofluorescence with antibodies to the centrosomal proteins  $\gamma$ -tubulin and kendrin. Left, merged images in which  $\gamma$ -tubulin is in red, kendrin in green, and DNA, as stained with Hoechst 33342, in blue. Scale bar, 10  $\mu$ m. (C) Percentage of control, FGD1-, golgin-84-, and GM130-depleted cells displaying more than four centrosomal foci (three independent experiments, with >300 cells counted per condition and per experiment).

organization was disrupted. Of interest, these latter factors did not affect Cdc42 activity at the Golgi, suggesting that the population of Cdc42 activity at the Golgi is independent of its PM-associated counterpart. Only Tuba controlled activity at the Golgi and the PM, which is likely due to its presence at both locations. It remains unclear whether Golgi-associated Cdc42 activity affects the population of this small GTPase at the PM.

The role of FGD1 at the Golgi is unclear. This GEF is reported to contribute to Cdc42 recruitment to the Golgi, but its depletion had no effect on the fraction of active, Golgi-associated Cdc42. It is possible that FGD1 at the Golgi may not be active or that it associates with inactive Cdc42. Alternatively, previous studies with FGD1 relied on overexpression of FGD1 mutants, which may have affected FGD1 function at the Golgi (Egorov *et al.*, 2009). Although additional experiments are needed to better understand the Golgi-associated pool of FGD1, our results demonstrate a role for this GEF at the PM, which is consistent with the reported reduction of Cdc42 activity in total lysates of FGD1-depleted cells (Egorov *et al.*, 2009).

Of interest, Cdc42 activity at the PM depended on an intact Golgi ribbon. We manipulated Golgi organization in two ways. We removed GM130, which leads to disconnected Golgi ministacks, glycosylation defects, and delayed protein transport (Puthenveedu *et al.*, 2006; Marra *et al.*, 2007). We also depleted golgin-84, which induces extensive Golgi fragmentation and a general reduction in protein transport (Diao *et al.*, 2003). We do not yet know which

aspect of Golgi function is required to activate Cdc42 at the PM because GM130 or golgin-84 depletion may interfere with protein modification, sorting, or transport of Cdc42 itself or a specific regulator. A mechanism involving post-Golgi transport would be consistent with previous findings on the requirement for membrane trafficking for Cdc42 activation at the leading edge of cells (Osmani *et al.*, 2010).

Our results led to a revised model of Cdc42-mediated regulation of the centrosome. We previously proposed that Cdc42 activity at the Golgi controls centrosome organization because GM130-depleted cells displayed reduced Cdc42 activity in biochemical assays and centrosome defects (Kodani *et al.*, 2009). However, the spatial analysis of Cdc42 activity establishes a strong correlation between Cdc42 activity at the PM and centrosome regulation. Cells in which PM-associated Cdc42 activity was specifically reduced—for example, as a result of FGD1 or golgin-84 depletion, displayed abnormal centrosome morphology, with an increased number of kendrin foci but normal  $\gamma$ -tubulin organization. These experimental conditions had no effect on Cdc42 activity at the Golgi, suggesting that Golgi-associated Cdc42 does not contribute to the regulation of this adjacent organelle. This revised model is consistent with previous findings on abnormal centrosomes in cells that either lacked Tuba or expressed dominant-negative Cdc42 (Kodani *et al.*, 2009).

It is not known how PM-associated Cdc42 controls the centrosome. A possible mechanism involves microtubules, which are necessary for centrosome assembly and whose dynamics depend on binding of activated Cdc42 to the PAR complex at the PM (Young *et al.*, 2000; Etienne-Manneville and Hall, 2003). Consistent with this idea, microtubule depolymerization with low concentrations of nocodazole caused changes in centrosome organization that phenocopied the depletion of GM130 or golgin-84 (Dammermann and Merdes, 2002). Microtubule attachment to the PM also promotes tension, which helps position the centrosome (Burakov *et al.*, 2003). Alternatively, active Cdc42 may contribute to the activation of the PAR complex, possibly controlling the centrosomal localization of the PAR6 isoforms Par6 $\alpha$  and Par6 $\gamma$ , which are necessary for centrosome assembly (Kodani *et al.*, 2010; Dormoy *et al.*, 2013).

Baschieri *et al.* (2014) reported a role for GM130 in the control of Cdc42 activity at the Golgi, which contradicts our findings. They found that GM130-depleted HEK293T cells had reduced levels of active Cdc42 at the Golgi, whereas activity levels at the PM were unaffected. Their model suggests that GM130-mediated Cdc42 regulation does not involve a GEF but, instead, GM130 binding to RasGRF2, a known negative regulator of the small GTPase Ras (Fernández-Medarde and Santos, 2011). There are several possible explanations for the discrepancies between our findings and those of Baschieri *et al.* (2014). For example, they used a single-chain biosensor in which the Rho GDI-binding site in Cdc42 is blocked.

However, the GDI–Cdc42 interaction was recently found to be critical for the spatiotemporal regulation of Cdc42 activity (Hodgson *et al.* 2016). Furthermore, they performed FRET measurements with the acceptor photobleaching method after cell fixation, which is reported to affect small GTPase localization (Michaelson *et al.*, 2001). In addition, they relied on the expression of their Cdc42 biosensor to mark the Golgi instead of labeling it with a specific marker. Finally, they used different cell lines, with depletions of GM130 and the various Cdc42 GEFs in HEK293T but experiments with RasGRF in HeLa cells.

In our study, in contrast, we detected the fractional population of active Cdc42 at the Golgi and the PM in living U2OS cells, using a dual-chain biosensor that maintains GDI binding, and measured FRET with the phasor approach to FLIM. Focus in our study was given to the specific locations of our FRET measurements, which were determined through coexpression of markers and only on cells in which manipulations were confirmed. Attempts to corroborate the results of Baschieri *et al.* (2014) were unsuccessful. We were unable to detect RasGRF2 in U2OS and HeLa cells by immunofluorescence or Western blot with the reported antibody (sc-863 C18; Santa Cruz Biotechnology) or two other commercial antibodies (sc-224 C-20, ProteinTech; 19717-1-AP; Santa Cruz Biotechnology; unpublished data). We also failed to deplete RasGRF2 from HeLa or U2OS cells with the reported siRNA (SI04235147; Qiagen). Thus better reagents have to be developed to resolve the discrepancies between these two studies.

In conclusion, we used the phasor approach to FLIM-FRET and a biosensor with an intact GDI interaction domain to demonstrate for the first time how manipulations of cellular factors, including GEFs, GAPs, and structural Golgi proteins, affect Cdc42 activity at the Golgi and the PM in live cells. Future studies will focus on understanding how Golgi organization and/or function controls Cdc42 activation at the PM and how active Cdc42 at the PM in turn regulates the centrosome. The assay and cell lines that we developed will help develop a comprehensive model of Cdc42 regulation at the Golgi, the PM, and other cellular locations.

## MATERIALS AND METHODS

### Molecular biology

The Cdc42-FLARE biosensor was based on the dual-chain biosensors described in Machacek *et al.* (2009). Cerulean fluorescent protein (CFP; Rizzo *et al.*, 2004) replaced CyPet to improve brightness and FRET efficiency, and residues 201–293 of WASP were used as the affinity reagent. The two biosensor chains were expressed on one open reading frame with two consecutive 2A viral peptide sequences from porcine teschovirus-1 (P2A) and *Thosea asigna* virus (T2A) inserted between them, leading to the production of two chains during translation (Kim *et al.*, 2011). The biosensor is undergoing further optimization, which will be described in detail in a separate publication. For the establishment of stable Cdc42-FLARE cell lines, we used the PiggyBac (PB) all-in-one cumate expression system PB-Cuo-MCS-IRES-GFP-EF1-CymR-Puro (PBQM812A-1; Systems Biosciences) and EF1 constitutive active expression system PB-EF1-MCS-IRES-Neo (PB533A-2; Systems Biosciences). The constructs were generated as follows: *PB-CuRo-MCS-EF1-CymR-Puro*: PB-Cuo-MCS-IRES-GFP-EF1-CymR-Puro was digested with *XcmI*/*AvrII* to release IRES-GFP, followed by a Klenow and religation. *PB-Cdc42-FLARE*: the Cdc42-FLARE fragment was released from pTriEx-myc-Ypet-Cdc42-binding domain (CBD)-P2A-T2A-Flag-Cer-Cdc42 (provided by Klaus Hahn, University of North Carolina) with *NheI*/*BstBI* and inserted between *NheI*/*Clal* of PB-Cuo-MCS-EF1-CymR-Puro. *PB-ManII-mCherry*: ManII-mCherry cDNA (available in

the Suetterlin lab) was inserted between *EcoRI*/*NotI* of PB-EF1-MCS-IRES-Neo. *PB-GalT-mCherry*: mCherry cDNA was inserted between *NheI*/*NotI* in PB-EF1-MCS-IRES-Neo; then GalT cDNA was PCR amplified from pYFP-GalT (a generous gift from John Presley, McGill University, Montreal, Canada; Yilmaz Dejgaard *et al.*, 2007) and inserted between *SacI*/*NotI* 5' of the mCherry cDNA. *PB-mApple-p58*: mApple cDNA (a generous gift from Michael Davidson, Florida State University, Tallahassee, FL; Kremers *et al.*, 2009) was first inserted between *NheI*/*EcoRI* of PB-EF1-MCS-IRES-Neo; then p58 cDNA was PCR amplified from pYFP-p58 (a generous gift from John Presley; Yilmaz Dejgaard *et al.*, 2007) and inserted into *EcoRI* downstream of mApple using the Cold Fusion kit (Systems Biosciences). *ARHGAP10-myc*: The fragment encoding for amino acids 885–1346 of ARHGAP10, which contains the PH and GAP domains, was amplified from the KIAA1424 template (Nagase *et al.*, 2000) and cloned into the *EcoRI* site of PCDNA3.1+.

### RNA interference

Protein depletion was carried out by transfecting U2OS cells (HTB96; American Type Culture Collection [ATCC]) with 200 nM (GM130, golgin-84, and scrambled) or 50 nM (Tuba, FGD1, and scrambled) siRNA duplexes using Oligofectamine as described by the manufacturer. The following sequences were used to target GM130: 5'-AAGT-TAGAGAGATGACGGAATC-3' (Puthenveedu *et al.*, 2006), Tuba: 5'-GAGCTTGAGGGAACATACAAGATT-3' (Kodani *et al.*, 2009), golgin-84: 5'-AAGTAGGATCTCGGACACCAG-3' (Diao *et al.*, 2003), FGD1-*Smartpool* (M-009612-01-0005; Dharmacon), and a scrambled control sequence, 5'-AAACTAACTGAGGCAATGCC3' (Sutterlin *et al.*, 2005). All siRNA duplexes were obtained from Life Technologies unless noted otherwise.

### Antibodies

Primary antibodies to the following proteins were used in this study: calreticulin (C4606; Sigma-Aldrich), Tuba (a gift from Frank Gertler, MIT; and B01P, Abnova), centrin2 (a gift from Jeffery L. Salisbury, Mayo Clinic; and Clone 20H5, Millipore), FGD1 (HPA 000911; Sigma-Aldrich), myc (Clone 9E10; Cal Biochem), GM130 (Clone 35; BD Biosciences; and G7295, Sigma-Aldrich), giantin (a gift from Vivek Malhotra, Center for Genomic Regulation, Barcelona, Spain), kendrin (a gift from Mikiko Takahashi, Teikyo Heisei University),  $\alpha$ -tubulin (T5168; Sigma-Aldrich),  $\gamma$ -tubulin (ab11310; Abcam), Cdc42 (Clone 44; BD Biosciences), and vesicular stomatitis virus G-protein (VSVG; BWG85; a gift from Victor Hsu, Harvard Medical School). Secondary antibodies for immunofluorescence were from Thermo Fisher or Biotium, and near-infrared antibodies for Western blots were from LI-COR (Lincoln, NE). For immunofluorescence, cells were fixed in either 100% ice-cold methanol (JT Baker) or 4% formaldehyde (Ted Pella), blocked and permeabilized with 2% blocking buffer (2% fetal bovine serum [FBS], 0.01% Triton X-100, and 1 $\times$  phosphate-buffered saline), stained with primary antibodies for 1 h at room temperature, and stained with secondary antibodies for 1 h. Coverslips were mounted with ProLong Gold (Thermo Fisher), and imaging dishes were filled with Ibidi Mounting Medium (Ibidi).

### Cell culture, establishment of stable cell lines, and protein expression

Parental U2OS cells (HTB96; ATCC) and all derived clonal cell lines were cultured in Advanced DMEM supplemented with 10% FBS (HyClone) and 2 mM GlutaMAX-I (GIBCO, Rockville, MD) at 37°C with 5% CO<sub>2</sub>. Stable cell lines were generated using the PB transposon system (System Biosciences). In brief, U2OS cells were cotransfected



with a PB-transposon construct (PB-mApple-p58, PB-GalT-mCherry, PB-ManII-mCherry, PB-mApple-Farnesyl, or PB-Cdc42-FLARE) and PB-transposase using X-tremeGENE 9 (Roche) as described by the manufacturer. Cells were selected for integration of the transposon using G418 at 500  $\mu\text{g}/\text{ml}$  or puromycin at 2  $\mu\text{g}/\text{ml}$  (Gold Biotechnology). Clonal cell lines were generated through serial dilution in 96-well plates.

Expression Cdc42-FLARE was accomplished by incubating the cells with 300  $\mu\text{g}/\text{ml}$  water-soluble cumate (Systems Bio Sciences) for 48 h. For transient transfections, DNA constructs were introduced into cells using Lipofectamine 3000 (Life Technologies) or X-treme Gene 9 according to manufacturer's protocol.

### FLIM-FRET experiment and analysis

**Cell preparation.** Inducible Cdc42-FLARE cell line was seeded in six-well dishes 60 h before imaging at 50% confluency. At 48 h before imaging, the cells were induced with 300  $\mu\text{g}/\text{ml}$  cumate (Systems Biosciences), and cumate concentration was maintained constant throughout the experiment. For protein depletion assays, 48 h before imaging, cells were transfected with RNAi using Oligofectamine. For protein expression, ~18 h before imaging, cells were transiently transfected with ARHGAP10 constructs using Lipofectamine 3000 (Life Technologies) or the cerulean control using X-treme Gene 9. At 24 h before imaging, cells were transferred to a  $\mu\text{Dish}^{35\text{ mm, high}}$  with Grid-500 (81166; Ibidi), which was used for live imaging and locating the previously imaged cells after fixation.

**Imaging.** All FLIM experiments were done in living cells, which were maintained at 37°C with 5%  $\text{CO}_2$ . After live imaging, cells were fixed, and the imaged cells were identified using the grid on the dish and analyzed using immunofluorescence to confirm protein depletion or expression. All data were acquired using a Zeiss LSM780 laser scanning microscope equipped with an incubation chamber and coupled to a two-photon Ti:sapphire laser (Spectra-Physics) and an ISS A320 FastFLIM box to acquire the lifetime data. An LD C-Apochromat 63 $\times$ /1.15 water immersion objective (Zeiss) was used for all live-cell experiments, and a Plan-Apochromat 63 $\times$ /1.40 Oil DIC was used for all fixed experiments. Cerulean was excited at 800 nm with 2.5% laser power from the two-photon laser pulsing at 80 fs at a repetition of 80 MHz. The laser light was separated from the fluorescence signal using an SP 760-nm dichroic filter. The fluorescence signal was directed through a 509 LP CFP/yellow fluorescent protein (YFP) filter; the signal was then split between two photomultiplier detectors (H7422P-40; Hamamatsu), equipped with either a CFP 470/22 or YFP 542/27 bandwidth filter. FLIM data were acquired with the SimFCS software developed at the Laboratory of Fluorescence Dynamics at the University of California, Irvine, with a dwell time of 25.61  $\mu\text{s}/\text{pixel}$  and the pixel frame size set to 256  $\times$  256, and the electronic zoom used to enhance resolution produced an image size of 24.53  $\times$  24.53  $\mu\text{m}$  (pixel size of ~100 nm). Fifty frames were collected per sample to limit exposure time to the laser to ~1.5–2 min. For each experiment, a solution of 50  $\mu\text{M}$  coumarin 6 (Sigma-Aldrich) dissolved in 100% ethanol was imaged as a calibration control. Zen Black 2012 (Zeiss) was used to control the microscope and collect confocal images of the mCherry/mApple cellular markers acquired in parallel with FLIM data and images of fixed cells.

**Data analysis.** FLIM data were processed to map the fraction of FRET for each cell using the SimFCS software (Laboratory of Fluorescence Dynamics, University of California, Irvine) as described

(Hinde *et al.*, 2012). In brief, files were calibrated against the coumarin 6 control, which has a known lifetime of 2.6 ns. The fluorescence lifetime of each pixel of the image was then mapped to the phasor plot. The lifetime of the cerulean in control cells and the autofluorescence signal were set on the phasor, and the FRET calculator in SimFCS was used to generate the FRET trajectory for mapping activity in cells. These measurements revealed a maximal detectable FRET efficiency of 28% for this biosensor. This maximal FRET efficiency was defined as 100% of the active Cdc42 population. Given that all of the FLIM images were collected for both donor and acceptor emission using a pixel of ~100 nm, ccRICS was performed with SimFCS to demonstrate that donor and acceptor proteins interacted in the selected regions of interest in biosensor-expressing cells. The cross-correlation method detects molecules of the two colors (donor and acceptor) diffusing together, also referred to as dynamic colocalization. In principle, cross-correlation does not demonstrate FRET but only that a complex is formed. In addition, the RICS method is sensitive to only diffusing molecules, with immobile molecules in the same pixel not contributing to the cross-correlation signal.

For intensity measurements, we used SimFCS to generate intensity histograms (photon counts/frame/pixel) for representative cells for each experimental condition.

To determine the average percentage of active Cdc42 at a specific location, we imported images of the Golgi or PM marker taken at the time of live imaging into Fiji using BioFormats and subjected them to thresholding using the IsoData method for the Golgi or hand tracing with a 20-pixel overlay brush for the PM (Ridler and Calvard, 1978; Linkert *et al.*, 2010; Schindelin *et al.*, 2012). These images were then imported into SimFCS and used to mask the FLIM data for the corresponding cell at the Golgi and the PM. To analyze the data, analysis of variance was created with post hoc *t* tests in R software.

For polarized cells, cells were divided into two regions by drawing a line through the nucleus perpendicular to the gradient (or where the gradient would have been in control cells) and then calculating the average Cdc42 activity for each region.

### Protein transport

VSVGts045-myc or VSVG-KDEL (a generous gift from Jennifer Lippincott-Schwartz, National Institutes of Health; Cole *et al.*, 1998) was transiently transfected into wild-type U2OS or U2OS-Cdc42-FLARE cells using X-treme Gene 9 and incubated at 37°C at 5%  $\text{CO}_2$  for 18 h. Before transport experiments, medium was supplemented with 25  $\mu\text{M}$  4-(2-hydroxyethyl)-1-piperazineethanesulfonic acid, pH 7.4. Cells were then incubated at 40.5°C for 4 h to accumulate VSVG in the ER, followed by a shift to the permissive temperature of 32°C to allow the protein to exit the ER. Cells were fixed in 4% formaldehyde (Ted Pella) at 0, 20, 60, or 120 min after shift to 32°C and processed for immunofluorescence analysis using an Axiovert 200 M microscope with AxioVision software (Zeiss). Cells with VSVG-KDEL were incubated for 2 h at 32°C to accumulate protein in the Golgi, followed by a shift to 37°C for 0, 2, 4, or 6 h to permit retrograde transport the ER. Image analysis was done with ImageJ.

### ACKNOWLEDGMENTS

We thank Susanne Rafelski, Rahul Warrior, and Grant MacGregor for helpful comments on the manuscript and John Presley, Michael Davidson, Frank Gertler, Jeffery L. Salisbury, Vivek Malhotra, Mikiko Takahashi, Victor Hsu, and Jennifer Lippincott-Schwartz for

generously providing reagents. This work was supported by Grant R01GM089913 from the National Institute of General Medical Sciences and Grants P41-GM103540 and P50-GM076516 (E.G. and M.A.D.) from the National Institutes of Health.

## REFERENCES

- Baschieri F, Confalonieri S, Bertalot G, Di Fiore PP, Dietmaier W, Leist M, Crespo P, Macara IG, Farhan H (2014). Spatial control of Cdc42 signaling by a GM130-RasGRF complex regulates polarity and tumorigenesis. *Nat Commun* 5, 4839.
- Benard V, Bokoch GM (2002). Assay of Cdc42, Rac, and Rho GTPase activation by affinity methods. *Methods Enzymol* 345, 349–359.
- Bhattacharya K, Swaminathan K, Peche VS, Clemen CS, Knyphausen P, Lammers M, Noegel AA, Rastetter RH (2016). Novel coronin7 interactions with Cdc42 and N-WASP regulate actin organization and Golgi morphology. *Sci Rep* 6, 25411.
- Burakov A, Nadezhdina E, Slepchenko B, Rodionov V (2003). Centrosome positioning in interphase cells. *J Cell Biol* 162, 963–969.
- Calvo F, Sanz-Moreno V, Agudo-Ibanez L, Wallberg F, Sahai E, Marshall CJ, Crespo P (2011). RasGRF suppresses Cdc42-mediated tumour cell movement, cytoskeletal dynamics and transformation. *Nat Cell Biol* 13, 819–826.
- Chen Y, Mills JD, Periasamy A (2003). Protein localization in living cells and tissues using FRET and FLIM. *Differentiation* 71, 528–541.
- Cole NB, Ellenberg J, Song J, DiEuliis D, Lippincott-Schwartz J (1998). Retrograde transport of Golgi-localized proteins to the ER. *J Cell Biol* 140, 1–15.
- Coso OA, Chiariello M, Yu JC, Teramoto H, Crespo P, Xu N, Miki T, Gutkind JS (1995). The small GTP-binding proteins Rac1 and Cdc42 regulate the activity of the JNK/SAPK signaling pathway. *Cell* 81, 1137–1146.
- Dammermann A, Merdes A (2002). Assembly of centrosomal proteins and microtubule organization depends on PCM-1. *J Cell Biol* 159, 255–266.
- Diao A, Rahman D, Pappin DJC, Lucocq J, Lowe M (2003). The coiled-coil membrane protein Golgin-84 is a novel rab effector required for Golgi ribbon formation. *J Cell Biol* 160, 201–212.
- Digman MA, Caiola VR, Zamai M, Gratton E (2008). The phasor approach to fluorescence lifetime imaging analysis. *Biophys J* 94, L14–L16.
- Dormoy V, Tormanen K, Suetterlin C (2013). Par6 gamma is at the mother centriole and controls centrosomal protein composition through a Par6 alpha-dependent pathway. *J Cell Sci* 126, 860–870.
- Dubois T, Paléotti O, Mironov AA, Fraiser V, Stradal TEB, de Matteis MA, Franco M, Chavrier P (2005). Golgi-localized GAP for Cdc42 functions downstream of ARF1 to control Arp2/3 complex and F-actin dynamics. *Nat Cell Biol* 7, 353–364.
- Egorov MV, Capestrano M, Vorontsova OA, Di Pentima A, Egorova AV, Mariggio S, Ayala MI, Tetè S, Gorski JL, Luini A, et al. (2009). Faciogenital dysplasia protein (FGD1) regulates export of cargo proteins from the Golgi complex via Cdc42 activation. *Mol Biol Cell* 20, 2413–2427.
- Elangovan M, Day RN, Periasamy A (2002). Nanosecond fluorescence resonance energy transfer fluorescence lifetime imaging microscopy to localize the protein interactions in a single living cell. *J Microsc* 205, 3–14.
- Erickson JW, Zhang CJ, Kahn RA, Evans T, Cerione RA (1996). Mammalian Cdc42 is a brefeldin A-sensitive component of the Golgi apparatus. *J Biol Chem* 271, 26850–26854.
- Estrada L, Caron E, Gorski JL (2001). Fgd1, the Cdc42 guanine nucleotide exchange factor responsible for faciogenital dysplasia, is localized to the subcortical actin cytoskeleton and Golgi membrane. *Hum Mol Genet* 10, 485–495.
- Etienne-Manneville S, Hall A (2001). Integrin-mediated activation of Cdc42 controls cell polarity in migrating astrocytes through PKCzeta. *Cell* 106, 489–498.
- Etienne-Manneville S, Hall A (2003). Cdc42 regulates GSK-3 $\beta$  and adenomatous polyposis coli to control cell polarity. *Nature* 421, 753–756.
- Fernández-Medarde A, Santos E (2011). The RasGrf family of mammalian guanine nucleotide exchange factors. *Biochim Biophys Acta* 1815, 170–188.
- Hanna S, Miskolci V, Cox D, Hodgson L (2014). A new genetically encoded single-chain biosensor for Cdc42 based on FRET, useful for live-cell imaging. *PLoS One* 9, e96469.
- Hehny H, Longhini KM, Chen J-L, Stamnes M (2009). Retrograde Shiga toxin trafficking is regulated by ARHGAP21 and Cdc42. *Mol Biol Cell* 20, 4303–4312.
- Hinde E, Digman MA, Welch C, Hahn KM, Gratton E (2012). Biosensor Förster resonance energy transfer detection by the phasor approach to fluorescence lifetime imaging microscopy. *Microsc Res Tech* 75, 271–281.
- Hodgson L, Spiering D, Sabouri-Ghomi M, Dagliyan O, DerMardirossian CEL, Danuser G, Hahn KM (2016). FRET binding antenna reports spatio-temporal dynamics of GDI-Cdc42 GTPase interactions. *Nat Chem Biol* 12, 802–809.
- Itoh RE, Kurokawa K, Ohba Y, Yoshizaki H, Mochizuki N, Matsuda M (2002). Activation of Rac and Cdc42 video imaged by fluorescent resonance energy transfer-based single-molecule probes in the membrane of living cells. *Mol Cell Biol* 22, 6582–6591.
- Kim JH, Lee SR, Li LH, Park HJ, Park JH, Lee KY, Kim MK, Shin BA, Choi SY (2011). High cleavage efficiency of a 2A peptide derived from porcine Teschovirus-1 in human cell lines, zebrafish and mice. *PLoS One* 6, e18556.
- Kodani A, Kristensen I, Huang L, Sütterlin C (2009). GM130-dependent control of Cdc42 activity at the Golgi regulates centrosome organization. *Mol Biol Cell* 20, 1192–1200.
- Kodani A, Tonthat V, Wu B, Sütterlin C (2010). Par6 alpha interacts with the dynactin subunit p150 Glued and is a critical regulator of centrosomal protein recruitment. *Mol Biol Cell* 21, 3376–3385.
- Kremers G-J, Hazelwood KL, Murphy CS, Davidson MW, Piston DW (2009). Photoconversion in orange and red fluorescent proteins. *Nat Methods* 6, 355–358.
- Kroschewski R, Hall A, Mellman I (1999). Cdc42 controls secretory and endocytic transport to the basolateral plasma membrane of MDCK cells. *Nat Cell Biol* 1, 8–13.
- Ku GM, Yablonski D, Manser E, Lim L, Weiss A (2001). A PAK1-PIX-PKL complex is activated by the T-cell receptor independent of Nck, Slp-76 and LAT. *EMBO J* 20, 457–465.
- Kunida K, Matsuda M, Aoki K (2012). FRET imaging and statistical signal processing reveal positive and negative feedback loops regulating the morphology of randomly migrating HT-1080 cells. *J Cell Sci* 125, 2381–2392.
- Linkert M, Rueden CT, Allan C, Burel JM, Moore W, Patterson A, Loranger B, Moore J, Neves C, Macdonald D, et al. (2010). Metadata matters: access to image data in the real world. *J Cell Biol* 189, 777–782.
- Luna A, Matas OB, Martínez-Menárguez JÁ, Mato E, Durán JM, Ballesta J, Way M, Egea G (2002). Regulation of protein transport from the Golgi complex to the endoplasmic reticulum by CDC42 and N-WASP. *Mol Biol Cell* 13, 866–879.
- Machacek M, Hodgson L, Welch C, Elliott H, Pertz O, Nalbant P, Abell A, Johnson GL, Hahn KM, Danuser G (2009). Coordination of Rho GTPase activities during cell protrusion. *Nature* 461, 99–103.
- Marra P, Salvatore L, Mironov A, Di Campli A, Di Tullio G, Trucco A, Beznoussenko G, de Matteis MA (2007). The biogenesis of the Golgi ribbon: The roles of membrane input from the ER and of GM130. *Mol Biol Cell* 18, 1595–1608.
- Matas OB, Martínez-Menárguez JÁ, Egea G (2004). Association of Cdc42/N-WASP/Arp2/3 signaling pathway with golgi membranes. *Traffic* 5, 838–846.
- Michaelson D, Silletti J, Murphy G, D'Eustachio P, Rush M, Philips MR (2001). Differential localization of Rho GTPases in live cells: regulation by hypervariable regions and RhoGDI binding. *J Cell Biol* 152, 111–126.
- Monympenny J, Zicha D, Higashida C, Ocegüera-Yanez F, Narumiya S, Watanabe N (2009). Cdc42 and Rac family GTPases regulate mode and speed but not direction of primary fibroblast migration during platelet-derived growth factor-dependent chemotaxis. *Mol Cell Biol* 29, 2730–2747.
- Nagase T, Kikuno R, Ishikawa KI, Hirokawa M, Ohara O (2000). Prediction of the coding sequences of unidentified human genes. XVI. The complete sequences of 150 new cDNA clones from brain which code for large proteins in vitro. *DNA Res* 7, 65–73.
- Nalbant P, Hodgson L, Kraynov V, Touchkine A, Hahn KM (2004). Activation of endogenous Cdc42 visualized in living cells. *Science* 305, 1615–1619.
- Nobes CD, Hall A (1995). Rho, rac, and cdc42 GTPases regulate the assembly of multimolecular focal complexes associated with actin stress fibers, lamellipodia, and filopodia. *Cell* 81, 53–62.
- Osmani N, Peglion F, Chavrier P, Etienne-Manneville S (2010). Cdc42 localization and cell polarity depend on membrane traffic. *J Cell Biol* 191, 1261–1269.
- Park S-Y, Yang J-S, Schmider AB, Soberman RJ, Hsu VW (2015). Coordinated regulation of bidirectional COPI transport at the Golgi by CDC42. *Nature* 521, 529–532.

- Puthenveedu MA, Bachert C, Puri S, Lanni F, Linstedt AD (2006). GM130 and GRASP65-dependent lateral cisternal fusion allows uniform Golgi-enzyme distribution. *Nat Cell Biol* 8, 238–248.
- Ridler TW, Calvard S (1978). Picture thresholding using an iterative selection method. *IEEE Trans Syst Man Cybernet* 8, 630–632.
- Rizzo MA, Springer GH, Granada B, Piston DW (2004). An improved cyan fluorescent protein variant useful for FRET. *Nat Biotechnol* 22, 445–449.
- Salazar MA, Kwiatkowski AV, Pellegrini L, Cestra G, Butler MH, Rossman KL, Serna DM, Sondek J, Gertler FB, de Camilli P (2003). Tuba, a novel protein containing bin/amphiphysin/Rvs and Dbl homology domains, links dynamin to regulation of the actin cytoskeleton. *J Biol Chem* 278, 49031–49043.
- Schindelin J, Arganda-Carreras I, Frise E, Kaynig V, Longair M, Pietzsch T, Preibisch S, Rueden C, Saalfeld S, Schmid B, *et al.* (2012). Fiji: an open-source platform for biological-image analysis. *Nat Methods* 9, 676–682.
- Sutterlin C, Polishchuk R, Pecot M, Malhotra V (2005). The Golgi-associated protein GRASP65 regulates spindle dynamics and is essential for cell division. *Mol Biol Cell* 16, 3211–3222.
- Wallrabe H, Chen Y, Periasamy A, Barroso M (2006). Issues in confocal microscopy for quantitative FRET analysis. *Microsc Res Tech* 69, 196–206.
- Wallrabe H, Periasamy A (2005). Imaging protein molecules using FRET and FLIM microscopy. *Curr Opin Biotechnol* 16, 19–27.
- Wu WJ, Erickson JW, Lin R, Cerione RA (2000). The gamma-subunit of the coatamer complex binds Cdc42 to mediate transformation. *Nature* 405, 800–804.
- Yilmaz Dejgaard S, Murshid A, Dee KM, Presley JF (2007). Confocal microscopy-based linescan methodologies for Intra-Golgi localization of proteins. *J Histochem Cytochem* 55, 709–719.
- Young A, Dichtenberg JB, Purohit A, Tuft R, Doxsey SJ (2000). Cytoplasmic dynein-mediated assembly of pericentrin and gamma tubulin onto centrosomes. *Mol Biol Cell* 11, 2047–2056.